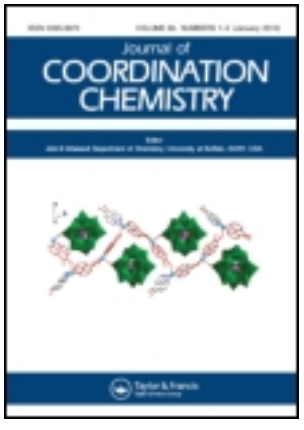

Journal of Coordination Chemistry
Publication details, including instructions for authors and subscription information:
http://www.tandfonline.com/loi/gcoo20

Three 5,5′-azotetrazolate-based cadmium(II) and zinc(II) complexes: syntheses, structures and photochromic and cell imaging properties

Wen-Bin Chen [a], Yan-Xuan Qiu [a], Xue-Mei Lin [a], Meng Yang [a], Hua Yan [a], Fei-Xian Gao [a], Zhen-Jie Ou Yang [a] & Wen Dong [a]
[a] Department of Chemistry, Guangzhou University, Guangzhou, P.R. China

Accepted author version posted online: 22 Mar 2013.Published online: 29 Apr 2013.

To cite this article: Wen-Bin Chen, Yan-Xuan Qiu, Xue-Mei Lin, Meng Yang, Hua Yan, Fei-Xian Gao, Zhen-Jie Ou Yang & Wen Dong (2013) Three 5,5′-azotetrazolate-based cadmium(II) and zinc(II) complexes: syntheses, structures and photochromic and cell imaging properties, Journal of Coordination Chemistry, 66:10, 1700-1708, DOI: 10.1080/00958972.2013.788157

To link to this article: http://dx.doi.org/10.1080/00958972.2013.788157

Journal of Coordination Chemistry, 2013
Vol. 66, No. 10, 1700–1708, http://dx.doi.org/10.1080/00958972.2013.788157

Three 5,5′-azotetrazolate-based cadmium(II) and zinc(II) complexes: syntheses, structures and photochromic and cell imaging properties

WEN-BIN CHEN, YAN-XUAN QIU, XUE-MEI LIN, MENG YANG, HUA YAN, FEI-XIAN GAO, ZHEN-JIE OU YANG and WEN DONG*

Department of Chemistry, Guangzhou University, Guangzhou, P.R. China

(*Received 6 December 2012; in final form 23 January 2013*)

Three 5,5′-azotetrazolate(AT)-based complexes, $[Cd(pn)_2(trans\text{-}AT)]$ (pn = 1,3-diaminopropane) (**1**), $[Cd(en)_2(trans\text{-}AT)]\cdot 4H_2O$ (en = ethylenediamine) (**2**), and $\{[Zn(en)_2(trans\text{-}AT)_{0.5}](trans\text{-}AT)_{0.5}\}$ (**3**), have been synthesized and characterized by single-crystal X-ray diffraction analysis. Complexes **1–3** show three different supramolecular structures, in which the trans-AT^{2-} have three different bridging modes. Complex **1** shows a 1-D zigzag chain structure formed by each μ_2-trans-AT^{2-} bridging two Cd^{2+} ions. In **2**, the trans-AT^{2-} anions are μ_2 bridging, linking Cd^{2+} ions to give another 1-D zigzag chain, which forms a 2-D supramolecular network by intermolecular hydrogen bonds. In **3**, $[Zn(en)_2(trans\text{-}AT)_{0.5}]^+$ forms a 2-D network structure with each μ_4 bridging trans-AT^{2-} linking four different Zn^{2+} ions. The $[Zn(en)_2(trans\text{-}AT)_{0.5}]^+$ and uncoordinated trans-AT^{2-} are further connected through face-to-face π–π stacking and electrostatic interactions, rendering a 3-D supramolecular network. The photochromism of aqueous solutions of **1–3** and $[Na_2(trans\text{-}AT)(H_2O)_5]$ (**L**) and the photoluminescence in solid samples of **2** and **3** as well as onion cell imaging with **2–3** and **L** as labels have been studied and reported.

Keywords: 5,5′-Azotetrazolate; Complex; Photochromism; Cell imaging

1. Introduction

N-heterocyclic multidentate ligands, such as triazole, tetrazole, and their derivatives, are widely employed to assemble 3d or 4f supramolecular complexes in inorganic–organic hybrid multifunctional materials [1–9]. N-heterocyclic azo compounds attract attention for fascinating structures, photochromism, bathochromic absorption, near-infrared luminescence, and application in photonic and memory storage devices [10–20]. Generally, azotetrazole, azotriazole, and their derivatives attract attention in study of energetic compounds [21–23]. Very recently, the photochromism of 1,1′-azobis-1,2,3-triazole and 1,1′-azobis-tetrazole was reported [10, 11]. The photochromism and photoluminescence of deprotonated 5,5′-azotetrazolae$(AT)^{2-}$-based transition metal complexes have also been reported by our group [14, 24]. AT^{2-} can undergo trans-to-cis isomerization upon UV–Vis or laser light irradiation (scheme 1). In crystal engineering, AT^{2-} is a good building block because it can control the crystal structure by simultaneously using different coordinating and

*Corresponding author. Email: dw320@yahoo.com.cn

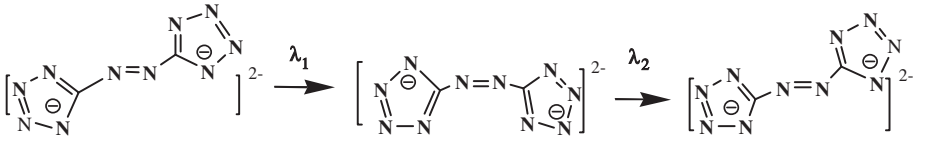

Scheme 1. Two consecutive isomerization process of AT^{2-}.

bridging modes as well as complementary intermolecular hydrogen bonding, π–π stacking, and electrostatic interactions in diverse environments. Numerous fluorescent molecules have been applied to labeling of biomolecules by forming covalent and noncovalent linkages [25–27]. Onion cell imaging is frequently studied because onions are readily available and their cells provide a clear view of all the basic characteristics of plant cell structure. Here, the crystal structures of **1–3** and **L**, their optical properties, and onion cell imaging with them as labels are reported and discussed.

2. Experimental

2.1. *Materials and physical measurements*

All commercial reagents and solvents are used without purification unless otherwise stated. IR spectra were recorded as pressed KBr pellets on a Bruker Tensor 27 spectrophotometer. Elemental analyses were carried out using a Perkin–Elmer analyzer model 240. UV–Vis absorption spectra of **1–3** and **L** in aqueous solution were recorded with a U-1800 UV–Vis spectrophotometer. The excitation and emission spectra of the solid sample were recorded on a F-4500 fluorescence spectrophotometer.

2.2. *Preparation of L and 1–3*

2.2.1. Synthesis of $[Na_2(trans\text{-}AT)(H_2O)_5]$ (L). $[Na_2(trans\text{-}AT)(H_2O)_5]$ (**L**) was synthesized according to reported method [28]. The crystallographic structure is shown in Supplementary material. Complexes of 5,5′-azotetrazole and its deprotonated anions are potentially explosive and should be handled in small quantities.

2.2.2. Synthesis of $[Cd(pn)_2(trans\text{-}AT)]$ (1). The 10 mL aqueous solution of $[Na_2(trans\text{-}AT)(H_2O)_5]$ (25.4 mg, 0.1 mM) was added to $CdCl_2{\cdot}2H_2O$ (21.9 mg, 0.1 mM) in 10 mL ethanol with stirring and a yellow precipitate formed. Then, 14.8 mg (0.2 mM) of pn was slowly added to the above mixture, and the yellow precipitates slowly dissolved giving a yellow solution. The yellow solution was heated and stirred for 1 h, filtered, and yellow crystals were obtained by slow evaporation of the filtrate for several days. The yellow crystals were washed with EtOH and the yield based on Cd^{2+} is about 67%. IR (KBr, cm^{-1}): 3309s, 33262s, 2937m, 2888s, 1586s, 1441w, 1389s, 1281m, 1195m, 1167s, 1143s, 999s, 902s, 735m, 610m, 559m. Elemental analysis: Anal. Calcd (%) for **1** $C_8H_{20}CdN_{14}$, Mr = 424.79: C, 22.58; H, 4.70; N, 46.12. Found (%): C, 22.31; H, 5.02; N, 46.27.

2.2.3. Synthesis of $[Cd(en)_2(trans\text{-}AT)]{\cdot}4H_2O$ (2). The synthesis of **2** was carried out in a method similar to that for **1** with en (12.0 mg, 0.2 mM) instead of pn. Yellow crystals

were obtained and the yield based on Cd^{2+} is 75%. IR (KBr, cm^{-1}): 3362s, 3306s, 2894m, 1603m, 1583m, 1401s, 1142w, 1033m, 971s, 731m, 632w. Elemental analysis: Anal. Calcd. (%) for **2** $C_6H_{24}CdN_{14}O_4$, Mr = 468.80: C, 15.36; H, 5.12; N, 41.81. Found (%): C, 15.31; H, 5.32; N, 41.67.

2.2.4. Synthesis of {[Zn(en)$_2$(trans-AT)$_{0.5}$] (trans-AT)$_{0.5}$} (3). The synthesis of **3** was similar to that for **2** using $ZnCl_2 \cdot 4H_2O$ (20.0 mg, 0.1 mM) instead of $CdCl_2 \cdot 2H_2O$ (21.9 mg, 0.1 mM). Yellow crystals were obtained and the yield based on Zn^{2+} is 76%. IR (KBr, cm^{-1}): 3334s, 3263m, 1624w, 1586m, 1498w, 1392s, 1002s, 734m, 658m, 506m. Elemental analysis: Anal. Calcd (%) for **3** $C_6H_{16}N_{14}Zn$, Mr = 349.72: C, 20.59; H, 4.57; N, 56.04. Found (%): C, 20.41; H, 4.71; N, 56.17.

2.3. *Fluorescence imaging experiments*

The lamellae suitable for microscopy experiments were prepared by coating the powder sample on cover glasses and drying in air. Imaging experiments were conducted with a laser scanning confocal microscope (LSCM) (510 META DUO SCAN) with oil-immersion objective lens 63× (NA = 1.4, Plan-Apochromat). The incident beam (408 nm) was split by beam splitter and focused into a small volume. The amplifier gain was set at 1.00, and the pixel time was 3.20 µs. For the plane imaging scan, green emission was collected with a 505–580 nm window.

2.4. *Onion cell fluorescence imaging experiments*

The onion samples were first immersed in 8% HCl for 5 min and washed with H_2O, then immersed in a 10^{-3} M dm^{-3} aqueous solution of complex for 20 min and washed with H_2O. Imaging experiments were conducted with the LSCM (510 META DUO SCAN).

2.5. *X-ray crystallography and data collection*

The crystals were filtered from the solution and immediately coated with a hydrocarbon oil on the microscope slide. Suitable crystals were mounted on glass fibers with silicone grease and placed in a Bruker Smart APEX(II) area detector using graphite monochromated MoK radiation ($\lambda = 0.71073$ Å) at 296(2) K. The crystallographic structures were solved by direct methods and successive Fourier difference syntheses (SHELXS-97) and refined by full-matrix least squares on F^2 with anisotropic thermal parameters for all nonhydrogen atoms (SHELXL-97) [29]. Hydrogens were added theoretically as riding on their parent atoms. Table 1 gives the crystal data and data collection parameters for **1–3**.

3. Results and discussion

3.1. *Crystal structures*

3.1.1. The crystal structure of [Cd(pn)$_2$(trans-AT)] (1). The atomic labeling diagram of **1** is shown in figure 1(a). Complex **1** crystallizes in the triclinic space group $P\bar{1}$. In **1**,

Table 1. The crystal data and data collection parameters for **1–3**.

	1	**2**	**3**
Formula	$C_8H_{20}CdN_{14}$	$C_6H_{24}CdN_{14}O_4$	$C_6H_{16}N_{14}Zn$
Mr	424.79	468.80	349.72
Crystal system	Triclinic	Triclinic	Triclinic
Space group	*Pī*	*Pī*	*Pī*
a/Å	6.985(2)	7.2961(9)	7.2384(3)
b/Å	8.284(3)	8.3402(10)	8.5517(3)
c/Å	8.354(3)	8.4053(10)	12.0049(7)
α/°	60.958(11)	73.040(5)	104.040(3)
β/°	66.111(12)	68.185(5)	97.207(3)
γ/°	74.649(13)	77.805(6)	105.047(2)
V/Å^3	385.0(2)	451.14(9)	681.97(5)
Z	1	1	2
D_c/g cm^{-3}	1.832	1.726	1.703
μ/ mm^{-1}	1.444	1.256	1.822
R^a	0.0127	0.0143	0.0241
$wR_2{}^b$	0.0333	0. 0378	0.0623

Table notes: $^aR = \sum F_o - F_c / \sum F_o$. $^bwR_2 = [\sum w(F_o^2 - F_c^2)^2 / \sum w(F_o^2)^2]^{1/2}$.

each Cd^{2+} coordinates to six nitrogens from two pn and two trans-AT^{2-} to form an octahedral geometry. The bond lengths of Cd(1)–N(3),Cd(1)–N(6), and Cd(1)–N(7) are 2.4208 (15), 2.3218(11), and 2.3620(17) Å, respectively. The axial N(3)–Cd(1)–N′(3) bond angle is 180°. In **1**, the trans-AT^{2-} is coplanar with dihedral angle of 0° between two tetrazolate rings. Each trans-AT^{2-} is a normal $\mu_{3,3'}$ bridge with N(3) and N′(3) from two different tetrazolate rings linking two different Cd^{2+} ions to give a 1-D zigzag chain structure (figure 1(b)) [24].

3.1.2. The crystal structure of $[Cd(en)_2(trans\text{-}AT)]\cdot 4H_2O$ (2). Figure 2(a) shows the atomic labeling diagram of **2**. Complex **2** crystallizes in the triclinic space group *Pī*. Each Cd^{2+} in **2** coordinates to six nitrogens from two en molecules and two trans-AT^{2-} in octahedral geometry. The bond lengths of Cd(1)–N(1), Cd(1)–N(6), and Cd(1)–N(7) are 2.4416(13), 2.3630(1), and 2.3468(11) Å, respectively. The N(1)–Cd(1)–N′(1) axial bond angle is 180°, and the trans-AT^{2-} is coplanar with dihedral angle of 0° between two tetrazolate rings. Each trans-AT^{2-} is a $\mu_{1,1'}$ bridge using N(1) and N′(1) linking two different Cd^{2+} ions to give another 1-D zigzag chain. Two O–H···N and O–H···O hydrogen bonds between noncoordinated N(2), N(4), N′(2), and N′(4) from each trans-AT^{2-} and waters with O···N distance of 2.941 Å and O···O distance of 2.872–2.957 Å result in a 2-D supramolecular network (figure 2(b)). A square tetrameric water cluster $(H_2O)_4$ is observed.

3.1.3. The crystal structure of $\{[Zn(en)_2(trans\text{-}AT)_{0.5}](trans\text{-}AT)_{0.5}\}$ (3). Single-crystal X-ray analysis reveals that **3** crystallizes in the triclinic space group *Pī*. Figure 3(a) shows the atomic labeling diagram of **3**. Each unit of **3** consists of a Zn^{2+}, half trans-AT^{2-}, and two en with half trans-AT^{2-} counter anion. In **3**, each Zn^{2+} coordinates to six nitrogens from two en and two trans-AT^{2-} to form an octahedron. The bond lengths are Zn(1)–N(4) = 2.3924(13), Zn(1)–N(6) = 2.1458(15), and Zn(1)–N(7) = 2.0840(13) Å and the axial bond

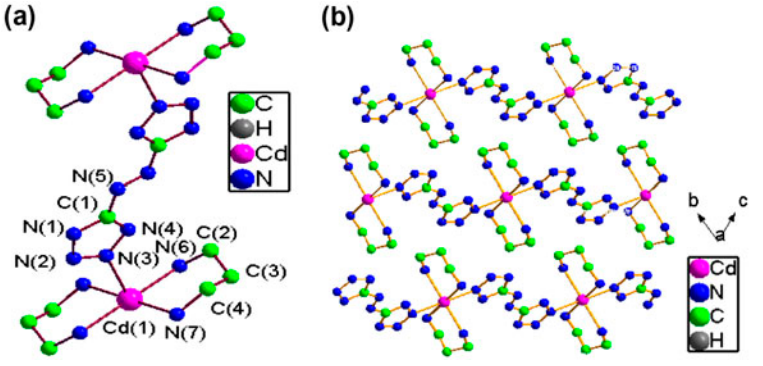

Figure 1. (a) The atomic labeling diagram of **1**. (b) The diagram of the 1-D zigzag chain structure in **1**.

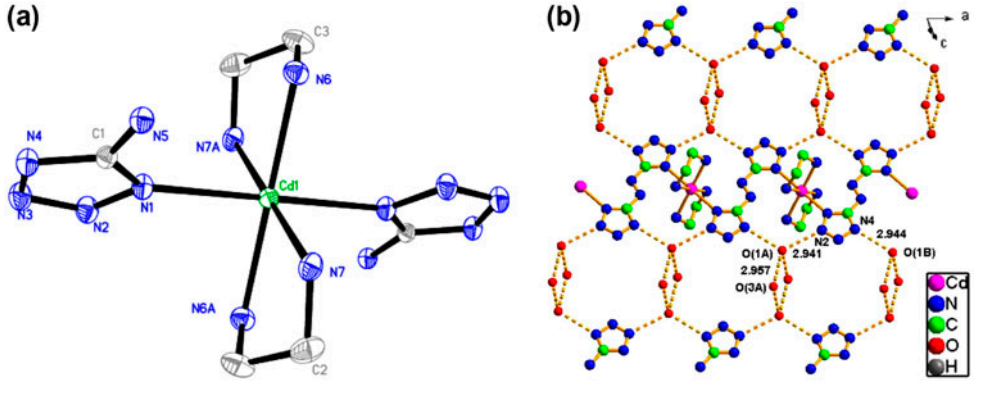

Figure 2. (a) The atomic labeling diagram of **2**. (b) The diagram of the O–H···N and O–H···O hydrogen bonds in **2**.

angle N(4)–Zn(1)–N(4A) = 180°. Each coordinating trans-AT^{2-} is a μ_4 bridge with N(2), N(4), N′(2), and N′(4) linking four different Zn^{2+} ions to give a 2-D network, showing a normal (6,3)-connected 2-D net with a long topological (O'Keeffe) vertex symbol of 666 (figure 3(b)). Both coordinating and noncoordinating trans-AT^{2-} are coplanar with dihedral angle of 0° between two tetrazolate anions. A slipped face-to-face anion-anion π–π stacking interaction was observed between two tetrazolate anionic rings from bridging and noncoordinating trans-AT^{2-} anions with interplanar center to center distances of 4.084 Å (figure 3(c)). The π–π stacking and electrostatic interactions link $[Zn(en)_2(trans\text{-}AT)]^+$ and the noncoordinating trans-AT^{2-} to give a 3-D supramolecular packing structure (figure 3(d)).

The molecular and supramolecular structures of 1–3 are different although the synthesizing conditions are similar; the reason may relate to the difference of pH in the reaction mixture and different steric effects of pn and en.

3.2. *The photochromism of 1–3 and L*

The UV–Vis spectral change of aqueous solution of **1** at 3.5×10^{-5} mol dm^{-3}, shown in figure 4(a), exhibits an intense π–π^* transition band at 309 nm with a molar extinction

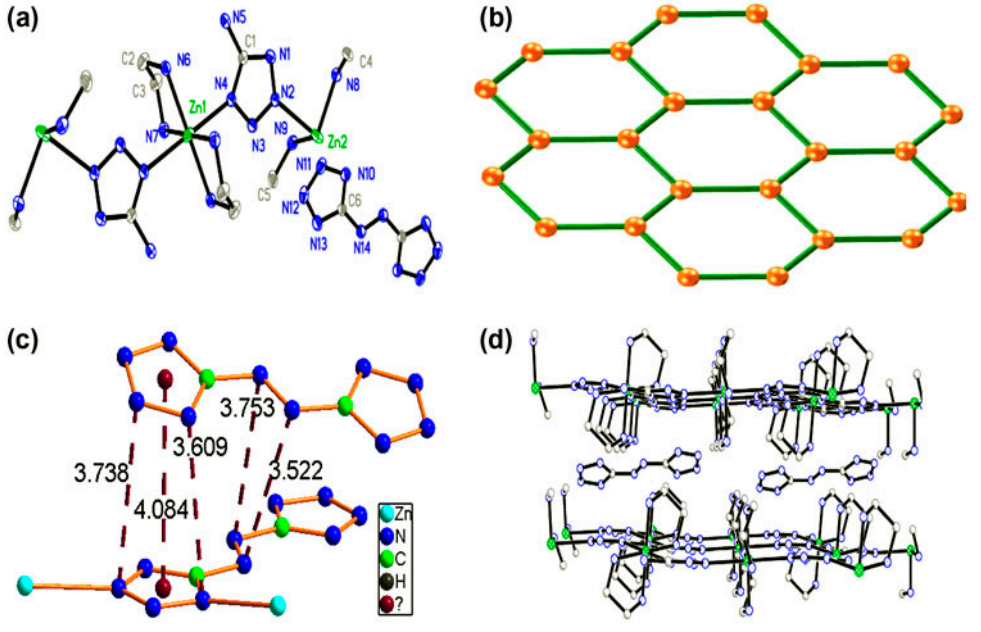

Figure 3. (a) The atomic labeling diagram of **3**. (b) The (6,3)-connected 2-D topological net for the complex unit of $[Zn(en)_2(trans\text{-}AT)]^+$ in **3** [orange sphere: $Zn(en)_2$; green sticks: trans-AT^{2-} anion. (c) The slipped face-to-face π–π stacking interaction. (d) The crystal packing diagram of **3**.

coefficient of $\varepsilon = 2.4 \times 10^4\,dm^3\,M^{-1}\,cm^{-1}$ and a weak n–π^* absorption at 416 nm with $\varepsilon = 1.1 \times 10^3\,dm^3\,M^{-1}\,cm^{-1}$ [14–16, 24]. Upon irradiation of the aqueous solution with UV light at 312 nm, the π–π^* band at 309 nm decreased in intensity with $\varepsilon = 1.9 \times 10^4\,dm^3\,M^{-1}\,cm^{-1}$ and the n–π^* band of the azo moiety at 416 nm increased in intensity with $\varepsilon = 1.7 \times 10^3\,dm^3\,M^{-1}\,cm^{-1}$ (the inset), suggesting that the trans isomer has converted to cis form in solution [10–19, 24, 30]. The aqueous solution of **L** at $4.2 \times 10^{-5}\,M\,dm^{-3}$ shows similar trans-to-cis isomerization with that of **1** (figure 4(b)). Under 312 nm UV light irradiation, the π–π^* band intensity at 309.5 nm decreased with ε changing from 1.7×10^4 to $1.2 \times 10^4\,dm^3\,M^{-1}\,cm^{-1}$ and n–π^* band intensity at 416 nm increased with ε changing from 5.5×10^2 to $1.0 \times 10^3\,dm^3\,M^{-1}\,cm^{-1}$. Both **2** and **3** show similar trans-to-cis isomerization in aqueous solution with the same concentration of **1** (Supplementary material).

3.3. *The solid photoluminescence of 2 and 3*

Figure 5(a) shows the room-temperature emission spectrum of the solid sample of **2** under 284 nm UV light excitation, and the inset shows the excitation spectrum of solid **2** with the monitored incident beam at 592 nm. **2** displays two emissive bands at 407 and 592 nm which should be attributed to radiative relaxation from excited states of trans-AT^{2-} [10, 11, 14]. Figure 5(b) displays the room-temperature emission spectrum of solid **3** under 281 nm UV light excitation, and the inset shows the excitation spectrum of solid **3** with the monitored incident beam at 377 nm. **3** displays three intense emissive peaks at 377,

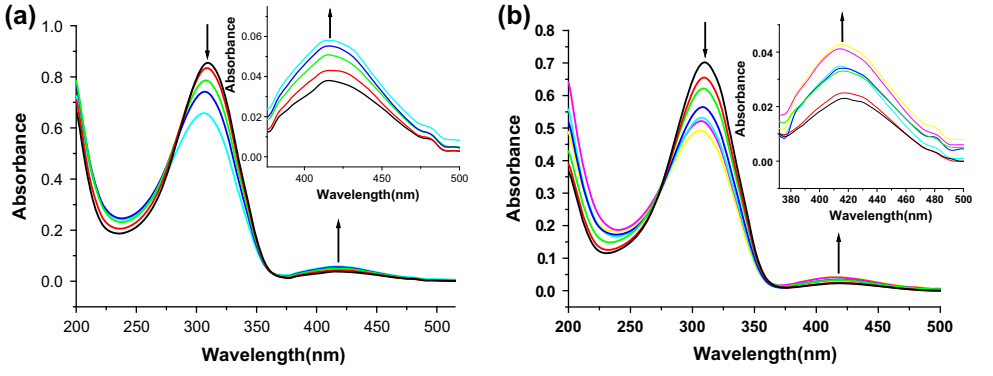

Figure 4. (a) UV–vis spectral change of **1** in aqueous solution with the concentration of 3.5×10^{-5} M dm^{-3} upon repeated irradiation at 312 nm at 2 min intervals at room temperature, (b) UV–vis spectral changes of **L** in aqueous solutions with the concentration of 4.2×10^{-5} M dm^{-3} upon repeated irradiation at 312 nm at 2 min intervals at room temperature.

557, and 627 nm. The bands at 377 and 557 nm should be attributed to radiative relaxation from the excited states of trans-AT^{2-}. However, it is difficult to assess the origins of the strong red Stokes shifted band at 627 nm [10, 11, 14].

3.4. *Photoluminescence of 2 and L under laser excitation*

Figure 6 shows the photoluminescent images of solid **2** taken by the LSCM. From the emission spectrum (figure 6(a)) corresponding to labeling position (figure 6(b)), **2** displays a green peak at 520 nm, a broad peak spanning green to orange regions from 560 and 605 nm and a main red emission peak around 650 nm under 408 nm laser excitation. The green (figure 6(c)) and red (figure 6(d)) confocal images are clearly distinguished by naked eyes, and the solid imaging indicates that **2** emits simultaneously green and red photoluminescence. These emission bands should be attributed to the radiative relaxation from the excited states of trans-AT^{2-} [10, 14]. Similarly, **L** also emits simultaneously green and red photoluminescence (Supplementary material).

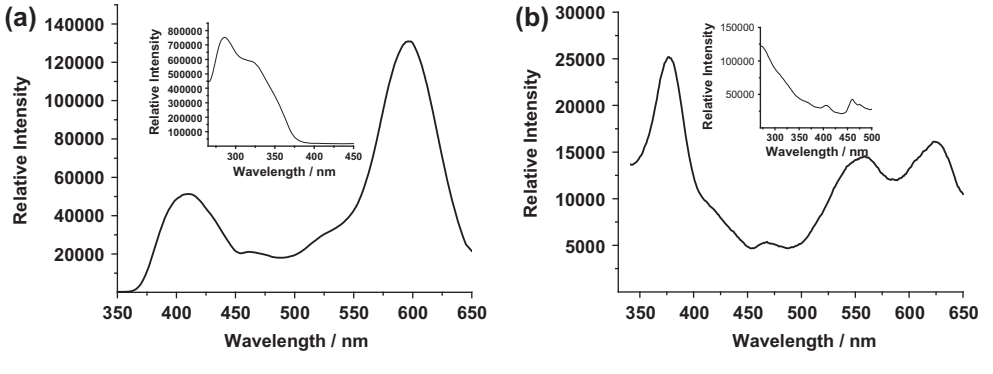

Figure 5. (a) Room-temperature emission spectrum of solid **2** under 284 nm irradiation (the inset shows the excitation spectrum of solid **2** with the monitored incident beam at 592 nm). (b) Room-temperature emission spectrum of solid **3** under 281 nm irradiation (the inset shows the excitation spectrum of solid **3** with incident beam at 377 nm).

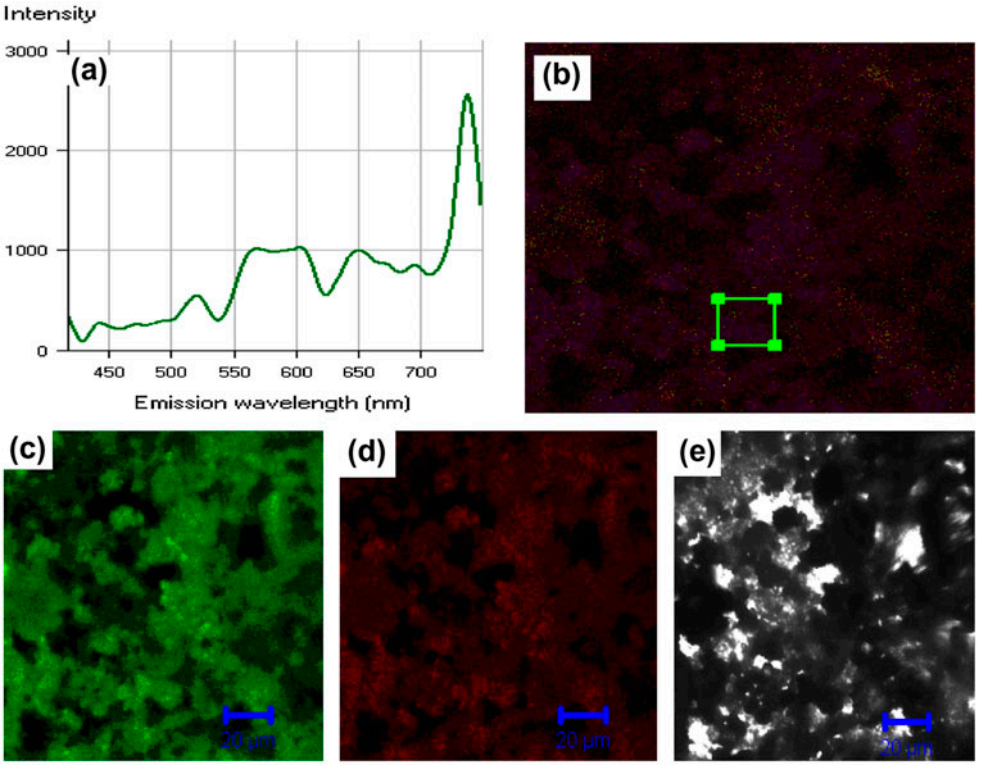

Figure 6. (a) The emission spectrum of solid **2** corresponding to labeling position, (b) confocal fluorescence images, (c) green image, (d) red image, (e) transparent image.

3.5. *The onion cell imaging*

The onion cell imaging using **2** as label under 408 nm laser excitation is provided in Supplementary Material. Clearly, the onion cell nucleus shows green and red imaging taken by LSCM after the sample was immersed in a 10^{-3} M dm^{-3} aqueous solution of two for 30 min. The green and red photoluminescence for onion cell nucleus originates from the radiative relaxation from the excited states of trans-AT^{2-} in **2**. The bioconjugate of onion cell nucleus to the fluorophore of **2** should be attributed to the intermolecular multiple hydrogen bonding interactions. The onion cell nucleus also exhibits green and red images using **3** and **L** as photoluminescent labels under 408 nm laser excitation (Supplementary material).

4. Conclusions

Three 5,5′-azotetrazolate-based complexes (**1–3**) have been reported and AT^{2-} shows three different coordinating and bridging modes. AT^{2-} can be employed to assemble varied supramolecular complexes. Aqueous solutions of **1–3** and **L** show similar photochromism. The solid samples of **2** and **L** emit simultaneously green and red photoluminescence and these complexes may be employed as new labels for onion cell imaging.

Supplementary material

Crystallographic data have been deposited in the Cambridge Crystallographic Database Center. CCDC reference numbers 764070 for **1**, 758556 for **2**, and 758558 for **3**. The data can be obtained free of charge from The Director, CCDC, 12 Union Road, Cambridge, CB21EZ, UK (Fax: t44 1223336 033; E-mail: deposit@ccdc.cam.ac.uk or http://www.ccdc.cam.ac.uk). The crystal packing diagram of $[Na_2(trans\text{-}AT)(H_2O)_5]$ (**L**), the UV–Vis spectral change of the aqueous solution of **2**, **3,** and the onion cell imaging using **3**, **L** as imaging agent under 408 nm laser excitation are shown in Supplementary material.

Acknowledgement

This work was supported by the National Natural Science Foundation of China (No. 21271052).

References

[1] J.S. Seo, D. Whang, H. Lee, S.I. Jun, J. Oh, Y. Jin, K. Kim. *Nature*, **404**, 982 (2000).
[2] O. Kahn, C.J. Martinez. *Science*, **279**, 44 (1998).
[3] R.-G. Xiong, X. Xue, H. Zhao, X.-Z. You, B.F. Abrahams, Z. Xue. *Angew. Chem. Int. Ed.*, **41**, 3800 (2002).
[4] M. Dincă, A.F. Yu, J.R. Long. *J. Am. Chem. Soc.*, **128**, 8904 (2006).
[5] L. Cheng, W.-X. Zhang, B.-H. Ye, J.-B. Lin, X.-M. Chen. *Inorg. Chem.*, **46**, 1135 (2007).
[6] X. He, C.-Z. Lu, D.-Q. Yuan. *Inorg. Chem.*, **45**, 5760 (2006).
[7] X.-S. Wang, Y.-Z. Tang, X.-F. Huang, Z.R. Qu, C.-M. Che, P.W.H. Chan, R.-G. Xiong. *Inorg. Chem.*, **44**, 5278 (2005).
[8] J.-M. Lin, B.-S. Huang, Z.-Q. Liu, D.-Y. Wang, W. Dong. *CrystEngComm*, **11**, 329 (2009).
[9] J.-M. Lin, Y.-F. Guan, W. Dong, X.-T. Wang, S. Gao. *Dalton Trans*., 6165 (2008).
[10] Y.-C. Li, C. Qi, S.-H. Li, H.-J. Zhang, C.-H. Sun, Y.-Z. Yu, S.-P. Pang. *J. Am. Chem. Soc.*, **132**, 12172 (2010).
[11] T.M. Klapötke, D.G. Piercey. *Inorg. Chem.*, **50**, 2732 (2011).
[12] Y. Li, B.O. Patric, D. Dolphin. *J. Org. Chem.*, **74**, 5237 (2009).
[13] O. Theilmann, W. Saak, D. Haase, R. Beckhaus. *Organometallics*, **28**, 2799 (2009).
[14] J.-M. Lin, W.-B. Chen, X.-M. Lin, A.-H. Lin, C.-Y. Ma, W. Dong, C.-E. Tian. *Chem. Commun.*, **47**, 2402 (2011).
[15] P. Pratihar, T.K. Mondal, A.K. Patra, C. Sinha. *Inorg. Chem.*, **48**, 2760 (2009).
[16] H. Nishihara. *Coord. Chem. Rev.*, **249**, 1468 (2005).
[17] S. Kume, H. Nishihara. *Dalton Trans*., 3260 (2008).
[18] J. Han, M. Maekawa, Y. Suenaga, H. Ebisu, A. Nabei, T. Kuroda-Sowa, M. Munakata. *Inorg. Chem.*, **46**, 3313 (2007).
[19] H.-S. Tang, N. Zhu, V.W.-W. Yam. *Organometallics*, **26**, 22 (2007).
[20] K. Higashiguchi, K. Matsuda, M. Irie. *Angew. Chem. Int. Ed.*, **42**, 3537 (2003).
[21] M.H.V. Huynh, M.A. Hiskey, E.L. Hartline, D.P. Montoya, R. Gilardi. *Angew. Chem. Int. Ed.*, **43**, 4924 (2004).
[22] G.H. Tao, B. Twamley, J.M. Shreeve. *Inorg. Chem.*, **48**, 9918 (2009).
[23] T.M. Klapötke, C.M. Sabaté. *Chem. Mater.*, **20**, 3629 (2008).
[24] J.-M. Lin, Y.-X. Qiu, W.-B. Chen, M. Yang, A.-J. Zhou, W. Dong, C.-E. Tian. *CrystEngComm*, **14**, 2779 (2012).
[25] M.S.T. Goncalves. *Chem. Rev.*, **109**, 190 (2009).
[26] N. Soh. *Sensors*, **8**, 1004 (2008).
[27] R.-G. Ute, G. Markus, C.-J. Sara, N. Roland, N. Thomas. *Nat. Methods*, **5**, 763 (2008).
[28] T.M. Klapotke, C.M. Sabate. *Chem. Mater.*, **20**, 3629 (2008).
[29] (a) G.M. Sheldrick, *SHELXS-97, Program for Solution of Crystal Structures*, University of Göttingen: Göttingen, Germany (1997); (b) G.M. Sheldrick, *SHELXL-97, Program for Refinement of Crystal Structures*, University of Göttingen, Göttingen, Germany (1997).
[30] K.K. Sarker, D. Sardar, K. Suwa, J. Otsuki, C. Sinha. *Inorg. Chem.*, **46**, 8291 (2007).